PROCEEDINGS OF SCIENCE

# Measurements of differential cross sections for W+jets and for multijet production and determination of the strong coupling constant in $p\bar{p}$ collisions at $\sqrt{s}$ = 1.96 TeV

**Michael Strauss***
*The University of Oklahoma, The D0 Collaboration*
*E-mail:* strauss@nhn.ou.edu

We present two sets of measurements based on data collected with the D0 detector at the Fermilab Tevatron collider running at $\sqrt{s} = 1.96$ TeV. First we present a comprehensive study of the differential cross sections for the production of $W$ bosons in association with up to four hadronic jets. Results are compared with the latest NLO and resummation theoretical predictions as well as with models implemented in event generators. We then present measurements of differential cross sections sensitive to multijet production, which are then interpreted in the framework of QCD to determine the evolution of the strong coupling constant in the energy range between 200 and 450 GeV, which has not been investigate yet in these type of studies.

*36th International Conference on High Energy Physics,*
*July 4-11, 2012*
*Melbourne, Australia*

*Speaker.

 

PoS(ICHEP2012)285

## 1. Introduction

The Fermilab Tevatron collides protons and anti-protons at a center of mass energy of 1.96 TeV. The D0 detector utilizes these collisions for studying Quantum Chromodynamics (QCD) the properties and interactions of quarks and gluons. Quarks and gluons are identified in the detector by their production of collimated "jets" of hadrons. The primary tool for measuring jets is the hadronic calorimeter [1]. Energy in the calorimeter is corrected to the particle level using the Jet Energy Scale (JES) which includes corrections for energy offset, detector response, out-of-cone showering and resolution. Comparison with theoretical predictions is done at the particle level which requires that a fragmentation model be applied to parton level calculations [2].

## 2. W + Jets Production

We present measurements of jet production in inclusive $W+(n)$ jet final states, with $n = 1$–4, using 3.8 fb$^{-1}$ of proton-antiproton collisions collected with the D0 detector. Measurements of $W+(n)$ jet final states are of interest because of the the important role they play in backgrounds to new physics and as multi-scale QCD processes.

Jets in the D0 detector are identified with the D0 RunII midpoint cone algorithm using a cone of radius $R_{\rm cone}$ = 0.5 to cluster calorimeter cells where $R = \sqrt{\eta^2+\phi^2}$, $\eta = -\ln(\tan(\theta/2))$, $\theta$ is the polar angle with respect to the proton beam direction, and $\phi$ is the azimuthal angle [3]. Electrons are identified as clusters of isolated calorimeter cells in which 95% of the energy in the shower is deposited in the electromagnetic (EM) section with a reconstructed charged particle track associated to the EM cluster. Events with a second isolated electron are removed to suppress the background from $Z$ boson and Drell-Yan production. The missing transverse energy, $\not\!\!E_T$, in the event is calculated as a vector sum of the calorimeter cell energies.

Selection criteria for electrons require that $p_T^e > 15$ GeV, $|\eta| < 1.1$, and $\Delta R > 0.5$. Selection criteria for jets require that there be at least one jet with transverse energy $E_T > 20$ GeV, and $|y| < 3.2$ where $y = 0.5\ln((E+p_z)/(E-p_z))$ where $p_z$ is the momentum along the proton beam direction. Each event is required to have the the primary vertex within 60 cm of the nominal vertex along the beam axis, $\not\!\!E_T < 20$ GeV, and $M_T^W > 40$ GeV, where $M_T^W$ is the invariant mass of the $W$ boson using the transverse energy and momentum of the electron and neutrino (the missing transverse energy). The background processes that are considered are $Z$+jets, $t\bar{t}$, single top, diboson, and multijet production. The signal and background processes are estimated using Monte Carlo samples excpet multijet production which is estimated using data.

Comparison of the data is made with different theoretical calculations: (1) Matrix element plus leading-order parton shower matched Monte Carlo event generator predictions from Sherpa 1.4.0 [4] with CT10 parton distribution functions (PDFs) [5], (2) All-order resummation predictions from High Energy Jets (HEJ) [6], (3) Next-to-Leading-Order (NLO) Blackhat+Sherpa predictions [7].

Results shown in Fig. 1 and 2 are normalised to the total inclusive $W$ cross-section in the defined phase space of the measurement in order to reduce systematic uncertainties on the measurement [8]. Fig. 1a shows the normalised differential production cross-sections of $W$ + $n$ jet events for $n$ = 1–4 as a function of $p_T(W)$ in each of the inclusive jet multiplicity bins. Data uncertainties include statistical and systematic uncertainties added in quadrature. Measured differential

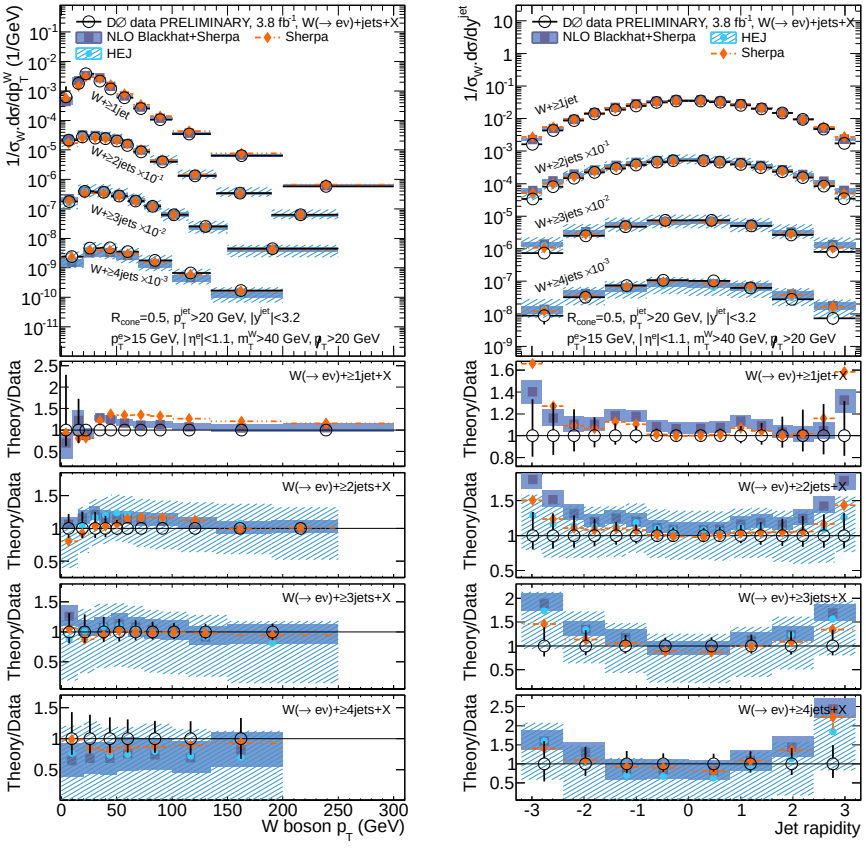


(a) (b)

**Figure 1:** Normalized unfolded differential production cross-sections measured as a function of (a) $W$ boson $p_T$, or (b) $n^{\text{th}}$ jet rapidities, in inclusive $W+n$ jet events. Lower panes show Theory/Data ratios for each of the $n$-jet multiplicity bin results separately.

production cross-sections as a function of the rapidity of the $n^{\text{th}}$ $p_T$-ordered jet in $W$ + ($n$) jet inclusive events are shown in Fig. 1b. Fig. 2 shows the dijet invariant mass distributions (formed from the two highest $p_T$ jets) in the two jet and three jet inclusive multiplicity bins in comparison with theoretical predictions. Fig. 3 shows the probability for additional jet emission (above a threshold of 20 GeV) in inclusive $W+2$ jet events studied as a function of dijet rapidity separation in three configurations: (1) rapidity separation between the two highest $p_T$ jets, (2) rapidity separation between the two highest $p_T$ jets with an additional requirement that the additional jet be emitted into the rapidity gap between the two highest $p_T$ jets, and (3) Rapidity separation of the most forward/backward jets. The first case has no additional requirement on where the third jet is emitted while the second case requires that the third jet be emitted in the rapidity region between the two highest $p_T$ jets. This distribution is sensitive to wide-angle soft gluon emission. The third case is an analogue of the second case but for rapidity-ordered jets, where rapidity intervals are generally larger, leading to stronger correlations and the ability to experimentally measure jet emission probabilities up to the highest rapidity separations. There is some indication that suppression of this jet emission rate begins to occur at the highest rapidity spans probed in this analysis. These results

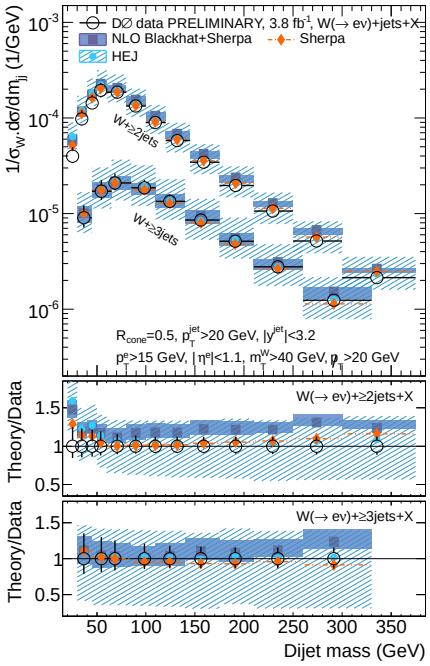


**Figure 2:** Normalized unfolded differential production cross-sections measured as a function of the invariant mass of the two highest $p_T$ jets in inclusive $W$ + 2 jet and $W$ + 3 jet events. Lower panes show Theory/Data ratios for each of the $n$-jet multiplicity bin results separately.

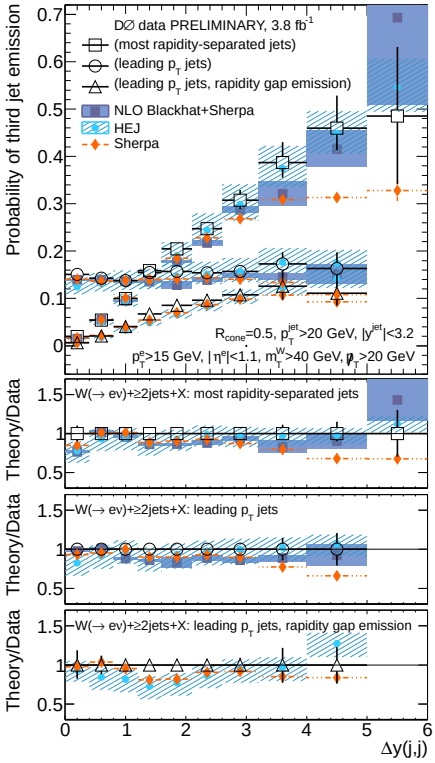


**Figure 3:** The probability of emission of a third jet in $W + 2$ jet events as a function of the dijet rapidity separation of (a) the two most rapidity separated jets ($p_T > 20$ GeV), (b) the two highest $p_T$ jets, (c) the two highest $p_T$ jets with the third jet emitted between these two jets in rapidity.

are the first of their kind for vector boson plus jet processes, and provide inputs to event generator modelling of widely separated jets.

## 3. Angular Correlation of Jets and Determination of $\alpha_s$

QCD predicts that the strong force between quarks and gluons becomes weaker when probed at high momentum transfers, corresponding to small distances. This property, referred to as asymptotic freedom, is derived from the renormalization group equation (RGE) [9]. The RGE does not predict the value of the strong coupling $\alpha_s$, but it describes its dependence on the renormalization scale $\mu_R$, and, therefore, on the momentum transfer. By convention, $\alpha_s$ values extracted from data at different momentum transfers are evolved to the common scale $\mu_R = M_Z$ to allow comparisons between experiments.

We introduce a new observable, $R_{\Delta R}$, for hadron-hadron collisions and measured its average value. It is related to the angular correlations of jets. In perturbative QCD (pQCD), this quantity is computed as a ratio of jet cross sections, which is proportional to $\alpha_s$. Since PDF dependencies

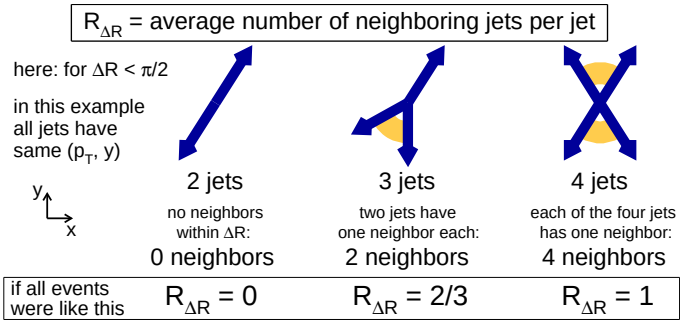


**Figure 4:** Selected examples of the value of $R_{\Delta R}$ for three different event types, assuming all events have the same topology.

largely cancel in the ratio, the extracted $\alpha_s$ results are almost independent of initial assumptions on the RGE. The measured quantity is the ensemble average over all jets in an inclusive jet sample, and is given by

$$R_{\Delta R}(p_T, \Delta R, p_{T\ \mathrm{min}}^{\mathrm{nbr}}) = \frac{\sum_{i=1}^{N_{\mathrm{jet}}(p_T)} N_{\mathrm{nbr}}^{(i)}(\Delta R, p_{T\ \mathrm{min}}^{\mathrm{nbr}})}{N_{\mathrm{jet}}(p_T)} \tag{3.1}$$

where $N_{\mathrm{jet}}(p_T)$ is the number of inclusive jets in a given inclusive jet $p_T$ bin, and $N_{\mathrm{nbr}}^{(i)}(\Delta R, p_{T\ \mathrm{min}}^{\mathrm{nbr}})$ is the number of neighboring jets with transverse momenta greater than $p_{T\ \mathrm{min}}^{\mathrm{nbr}}$ separated from the $i$-th inclusive jet by a distance $\Delta R$ within a specified interval $\Delta R_{\mathrm{min}} < \Delta R < \Delta R_{\mathrm{max}}$. For $\Delta R < 2\pi$, only topologies with at least three jets contribute to the numerator of Eq. 3.1 in pQCD and $R_{\Delta R}$ is proportional to $\alpha_s$. Fig. 4 shows different values of $R_{\Delta R}$ for three special cases with all events having the same jet topology.

This measurement is based on a data set corresponding to an integrated luminosity of 0.7 fb$^{-1}$ using jets found with the D0 Run II midpoint cone algorithm with $R_{\mathrm{cone}} = 0.7$ [3]. All jets with $|y| < 1$ and $p_T > 50$ GeV are used to find $R_{\Delta R}$. It is measured triple differentially, as a function of inclusive jet $p_T$, for different $p_{T\ \mathrm{nbr}}^{\mathrm{nbr}}$ requirements of 30, 50, 70, or 90 GeV, respectively, and in different $R_{\Delta R}$ intervals of $1.4 < \Delta R < 1.8$, $1.8 < \Delta R < 2.2$, and $2.2 < \Delta R < 2.6$.

The results for $R_{\Delta R}$ are displayed in Fig. 5 as a function of inclusive jet $p_T$ in different regions of $\Delta R$ and for different $p_{T\ \mathrm{nbr}}^{\mathrm{nbr}}$. The theory predictions for $R_{\Delta R}$, calculated at NLO, include correction factors for non-perturbative effects, including hadronization and underlying event. Most of the PDF dependencies cancel in the ratio. For $p_{T\ \mathrm{nbr}}^{\mathrm{nbr}} = 50$, 70, and 90 GeV, the theoretical predictions are in good agreement with data. For $p_{T\ \mathrm{nbr}}^{\mathrm{nbr}} = 30$ GeV the predictions are systematically below the data which might be caused by limitations of either the perturbative calculation or the modeling of the non-perturbative effects.

These $\Delta R$ results are then used to determine $\alpha_s$ and to test the two-loop RGE prediction for its running as a function of $p_T$ . In an initial study, the data are split into 12 subsets defined by the different $p_{T\ \mathrm{nbr}}^{\mathrm{nbr}}$ requirements. Assuming the RGE, the value of $\alpha_s(M_Z)$ is fitted to each of these subsets, and the corresponding $\chi^2$ values are determined that compare data and theory. Since each of these subsets covers a large inclusive jet $p_T$ range, a violation of the RGE would be reflected in poor $\chi^2$ values. The data from kinematic regions in $(\Delta R, p_{T\ \mathrm{nbr}}^{\mathrm{nbr}})$ which have fits that are consistent with each other are then used in the subsequent analysis. These data are split into 12 groups, each

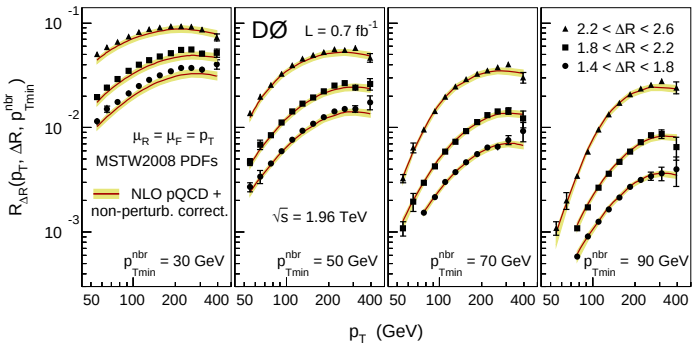


**Figure 5:** The measurement of $R_{\Delta R}$ as a function of inclusive jet $p_T$ for three different intervals in $\Delta R$ and for four different requirements of $p_{T\,\mathrm{nbr}}^{\mathrm{nbr}}$. The inner uncertainty bars indicate the statistical uncertainties, and the total uncertainty bars display the quadratic sum of the statistical and systematic uncertainties. The theory predictions are shown with their uncertainties.

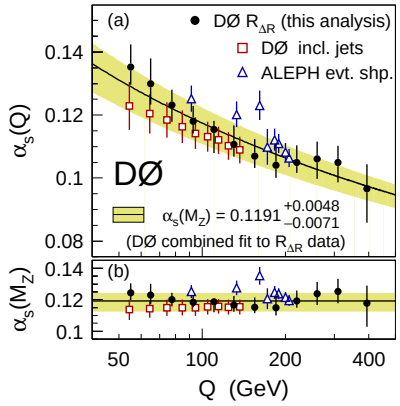


**Figure 6:** (a) The strong coupling $\alpha_s(Q)$ and the RGE prediction. (b) The $\alpha_s(M_Z)$ result from the fit and RGE for all selected data points. The uncertainty includes the experimental and theoretical contributions. Results from [11] and [12] are also shown.

with the same inclusive jet $p_T$, combining data points for different $(\Delta R, p_{T\,\mathrm{nbr}}^{\mathrm{nbr}})$. For each group, $\alpha_s$ is determined at the corresponding $p_T$ , and then evolved using the RGE, to $\mu_R = M_Z$.

All data points with the same $p_T$ (from all three $\Delta R$ regions and for $p_{T\,\mathrm{nbr}}^{\mathrm{nbr}}$ = 50, 70, and 90 GeV where the fits are good), are combined to fit $\alpha_s(Q)$, in the range $50 < Q < 450$ GeV where $Q$ is the momentum transfer, (Fig. 6). Using the RGE, the individual results are evolved to $\mu_R = M_Z$, and shown in Fig. 6b. A combined fit, using the same data set integrated over $p_T$, and for MSTW2008NLO PDFs [10], gives the result $\alpha_s(M_Z) = 0.1191^{+0.0048}_{-0.0071}$. The RGE prediction for this result is displayed in Fig. 6a. The $\alpha_s(p_T)$ results from $R_{\Delta R}$ are well described by the RGE prediction including the region $208 < \mu_R < 400$ GeV, in which the RGE is tested for the first time.

## References

[1] V.M. Abazov, et al., D0 Collaboration, Nucl. Instrum. Methods Phys. Res. A 565, 463 (2006).
[2] C. Buttar, et al., in: G. Belanger, et al. (Eds.), Les Houches 2007, Physics at TeV Colliders, arXiv:0803.0678 [hep-ph], Section 9.
[3] G. C. Blazey et al., in: U. Baur, R.K. Ellis, and D. Zeppenfeld, (Eds.), Fermilab-Pub-00/297 (2000).
[4] T. Gleisberg, et.al., JHEP 0902, 007 (2009).
[5] H.-L. Lai, M. Guzzi, J. Huston, et.al., Phys. Rev. D 82, 074024 (2010).
[6] J. R. Andersen and J. M. Smillie, JHEP 1001, 039 (2010); J. R. Andersen and J. M. Smillie, Nucl. Phys. Proc.Suppl. 205-206, 205 (2010); J. R. Andersen and J. M. Smillie, JHEP 1106, 010 (2011).
[7] C. F. Berger, Z. Bern, L. J. Dixon, et.al., Phys. Rev. Lett. 102, 222001 (2009); C. F. Berger, Z. Bern, L. J. Dixon, et.al., arXiv:0905.2735 [hep-ph].
[8] V. M. Abazov et al., D0 Collaboratin, Phys. Lett. B 705, 200 (2011)
[9] C.G. Callan Jr., Phys. Rev. D 2, 1542 (1970) 1541; K. Symanzik, Commun. Math. Phys. 18, 227 (1970); K. Symanzik, Commun. Math. Phys. 23, 49 (1971).
[10] A.D. Martin, et al., Eur. Phys. J. C 63, 18 (2009).
[11] V.M. Abazov, et al., D0 Collaboration, Phys. Rev. D 80, 111107 (2009).
[12] G. Dissertori, et al., J. High Energy Phys. 0908, 36 (2009).